Electronic Supplementary Material (ESI) for Organic & Biomolecular Chemistry.

Catalytic Mechanism of Mevalonate Kinase Revisited, a QM/MM Study

James McClory [†], Jun-Tang Lin [‡], David J. Timson[§], Jian Zhang[//], Meilan Huang[†,*]

[†] School of Chemistry and Chemical Engineering, Queen's University Belfast, David Keir Building, Stranmillis Road, Belfast, BT9 5AG, Northern Ireland, United Kingdom

[‡] Stem Cells and Biotheraphy Engineering Research Centre of Henan, College of Biomedical Engineering, Xinxiang Medical University, Xinxiang 453003, China

§ School of Pharmacy and Biomolecular Sciences, The University of Brighton, Huxley Building, Lewes Road, Brighton, BN2 4GJ, United Kingdom

[//] Shanghai Jiaotong University, 280 Chongqing Road, Shanghai 200025, China

Corresponding author

*Meilan Huang

Phone: +44 28 9097 4698

Fax: +44 28 9097 6524

E-mail: m.huang@qub.ac.uk

Table S1. The protonation states of histidine residues in MVK.

Residue	Protonation State
His17	HIE
His20	HIE
His24	HIE
His197	HIE
His303	HIE
His304	HIE
His312	HIE
His325	HIE
His328	HIE
His380	HIE

*HIE denotes Histidine with hydrogen on the epsilon nitrogen

Table S2. RESP charges of atoms in mevalonate of MVK

No.	Atom Name	Atom Type	RESP Charge
1	C1	CT	-0.23
2	C2	CT	0.53
3	C3	CT	-0.55
4	C4	CT	0.42
5	O1	OH	-0.74
6	H1	HO	0.42
7	O2	OH	-0.69
8	H2	HO	0.39
9	C5	CT	-0.65
10	C6	C	1.07
11	O3	O2	-0.87
12	O4	O2	-0.87
13	H3	HC	0.07
14	H4	HC	0.07
15	H5	HC	0.07
16	H6	HC	0.16
17	H7	HC	0.16
18	H8	H1	-0.01
19	H9	H1	-0.01
20	H10	HC	0.13
21	H11	HC	0.13

Table S3. Benchmark study on the basis set used for DFT (B97D) functional in the correction of the QM/MM calculated energies (kcal/mol) for the reaction catalyzed by MVK.

	Reactant	**TS**	**Product**
6-31g(d) Opt	0	17.1	5.4
6-31g(d,p) SP	0	17.1	4.6
6-31+g(d) SP	0	18.1	2.9
6-311++g(d,p) SP	0	17.9	1.8
6-311+g(2d,2p) SP	0	20.3	2.5

Table S4. Cluster analysis of the 100-ns MD simulations of the ATP-Mg^{2+}-MVK-MVA complex.

Cluster	Occurrence (%)	Distance MVA:C^5OH-ATP:γPO_3 (Å)
1	1.5	3.761
2	3.3	3.802
3	4.3	3.856
4	0.9	3.859
5	7.3	3.887
6	6.7	3.751
7	21.8	3.782
8	**33.6**	**3.819**
9	13.3	3.720
10	7.2	3.703

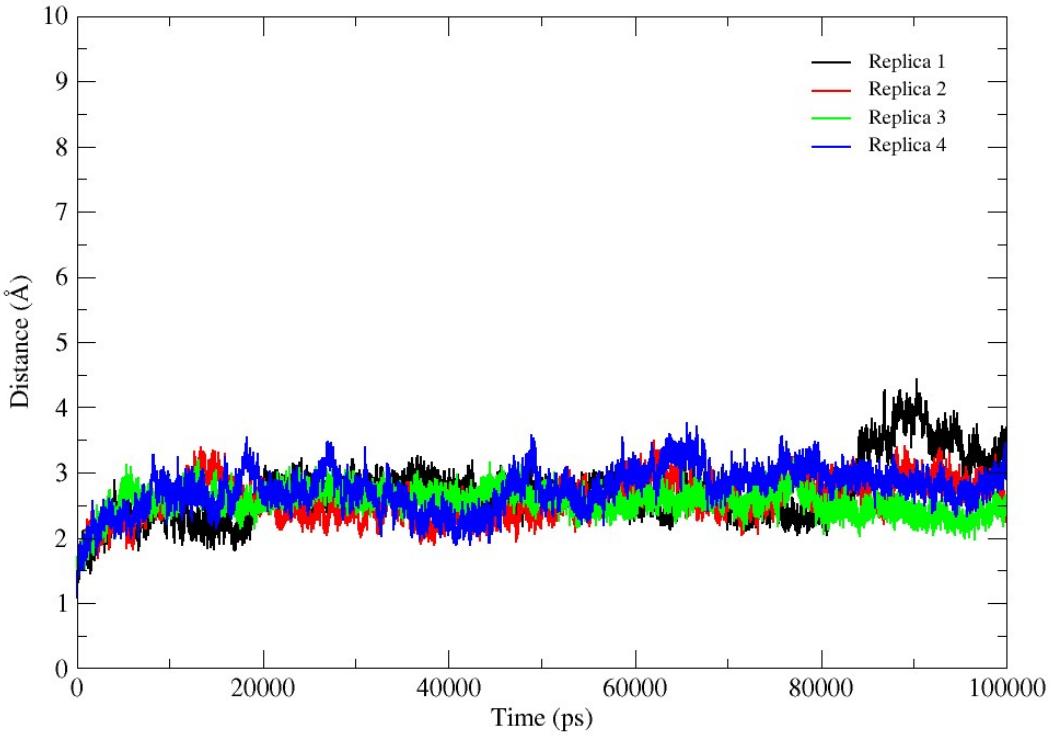

Figure S1. RMSD for the backbone Cα atoms of ATP- Mg^{2+}-MVK-MVA complex.

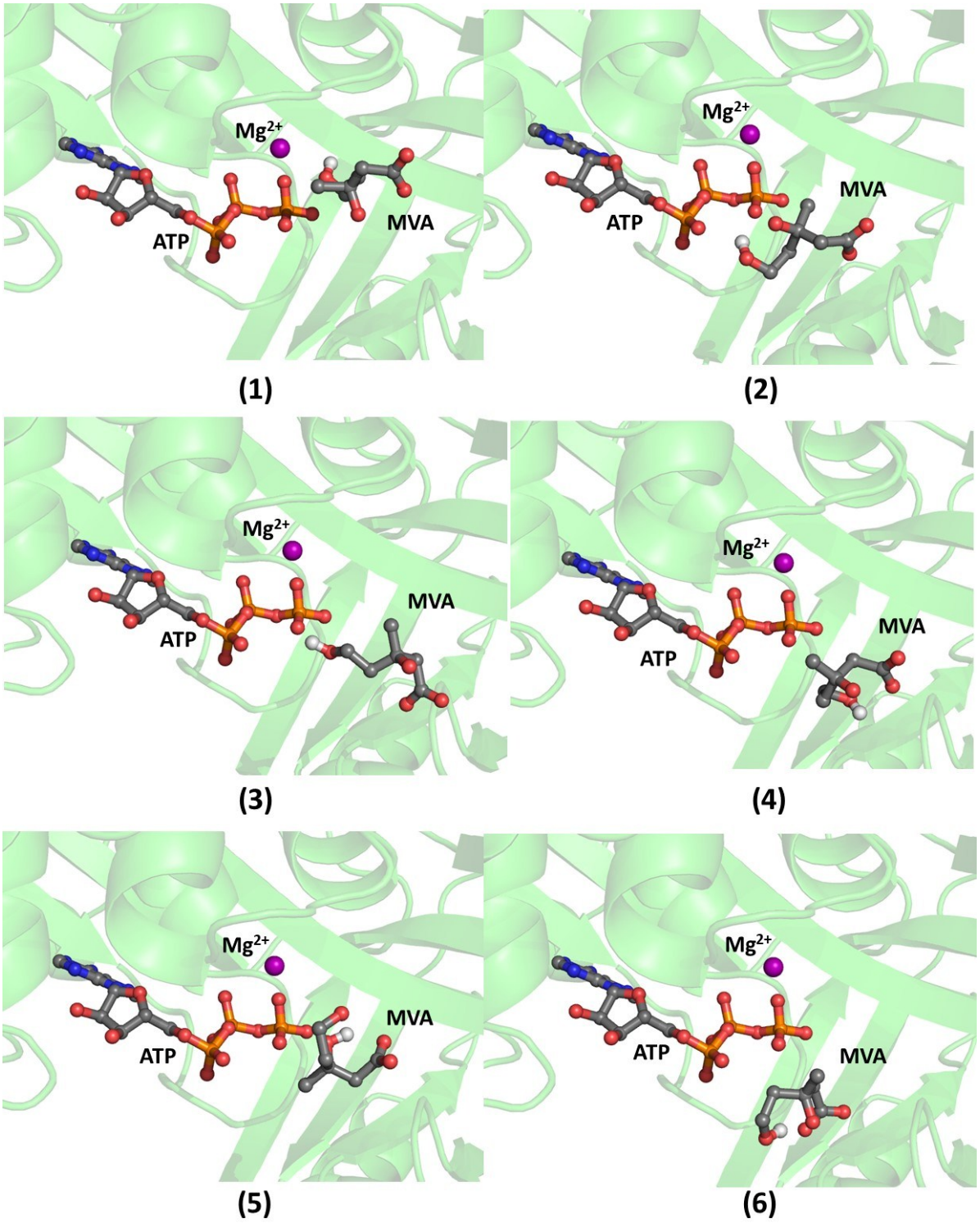

Figure S2. Docking poses of MVA in MVK.

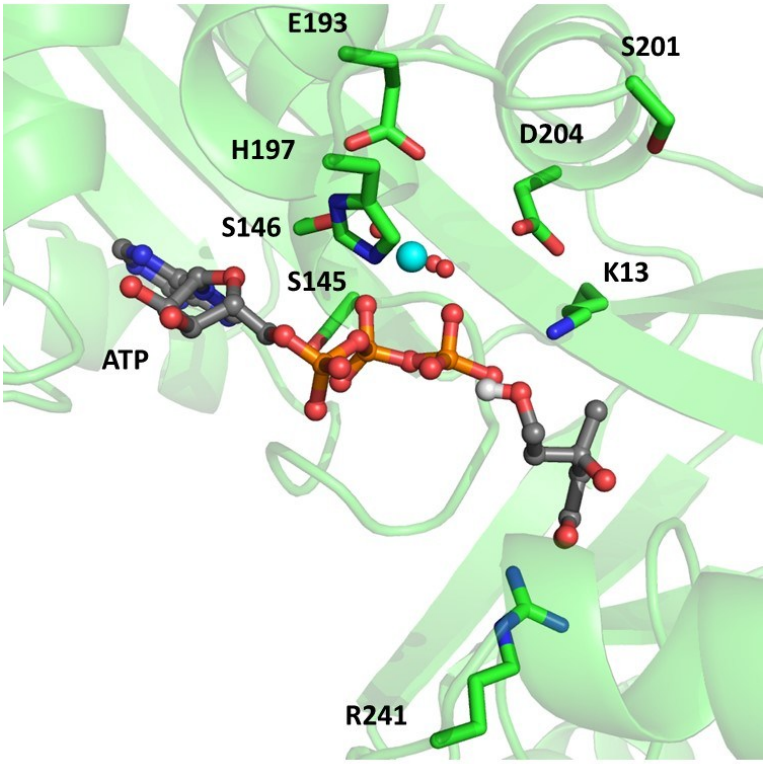

Figure S3. MD simulated structure of the ATP- Mg^{2+}-MVK -MVA model (inactive), built in analogy to the crystal structure of MVK in absence of substrate. In this model, Mg^{2+} is coordinated with the β- and γ-phosphate oxygen atoms of ATP.

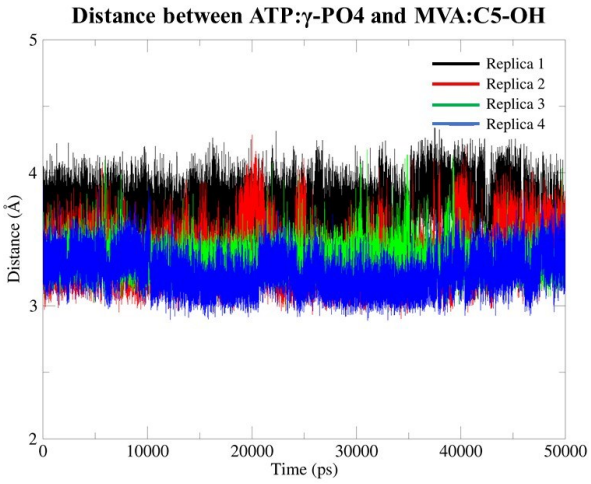

Figure S4. Distance from 4 replicas of 100-ns MD simulations of the ATP -Mg^{2+}-MVK-MVA complex (plotted based on the last 50 ns trajectory) between the carboxylate group of MVA and the γ-phosphate of ATP.

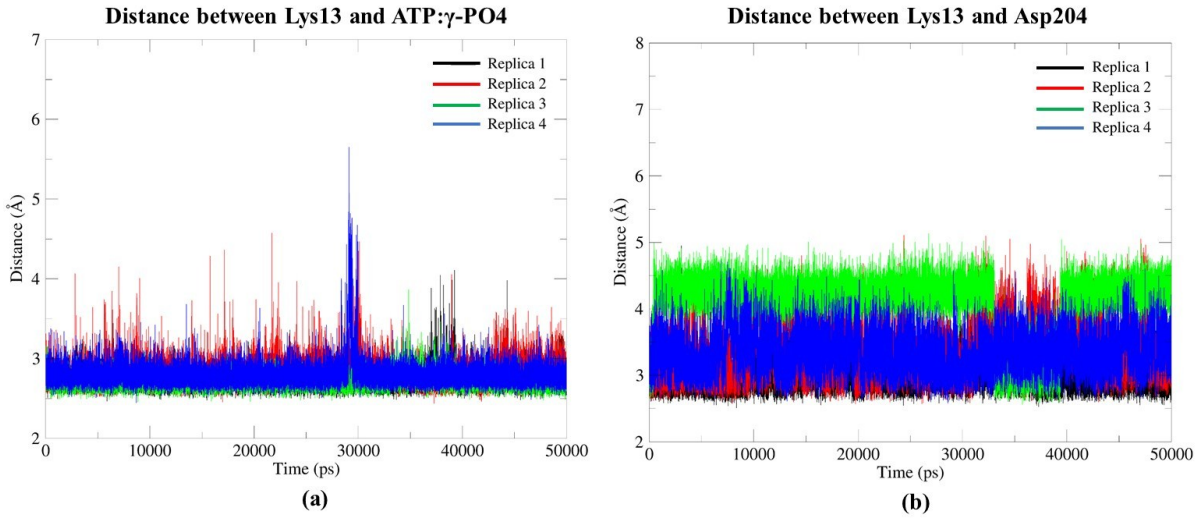

Figure S5. Distance from 4 replicas of 100-ns MD simulations of the ATP -Mg^{2+}-MVK-MVA complex (plotted based on the last 50 ns trajectory) (a) between Lys13 and γ-PO_4 of ATP; (b) between Lys13 and Asp204.

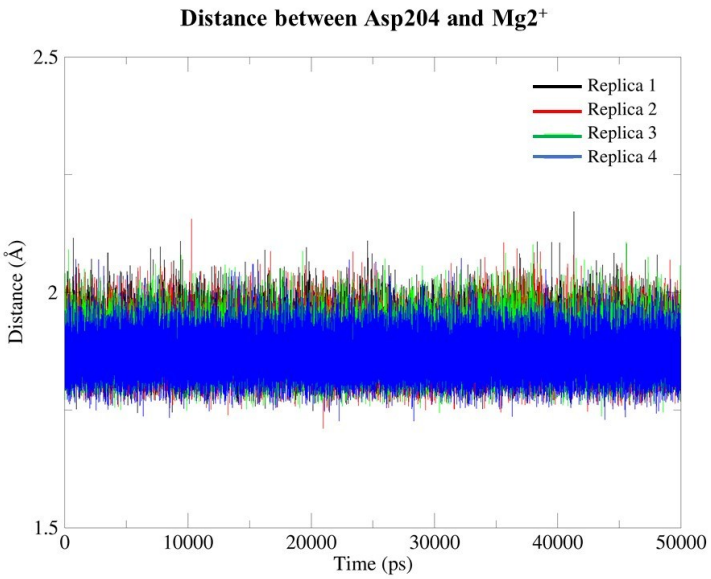

Figure S6. Distance from 4 replicas of 100-ns MD simulations of the ATP -Mg^{2+}-MVK-MVA complex (plotted based on the last 50 ns trajectory) between Asp204 and Mg^{2+}.

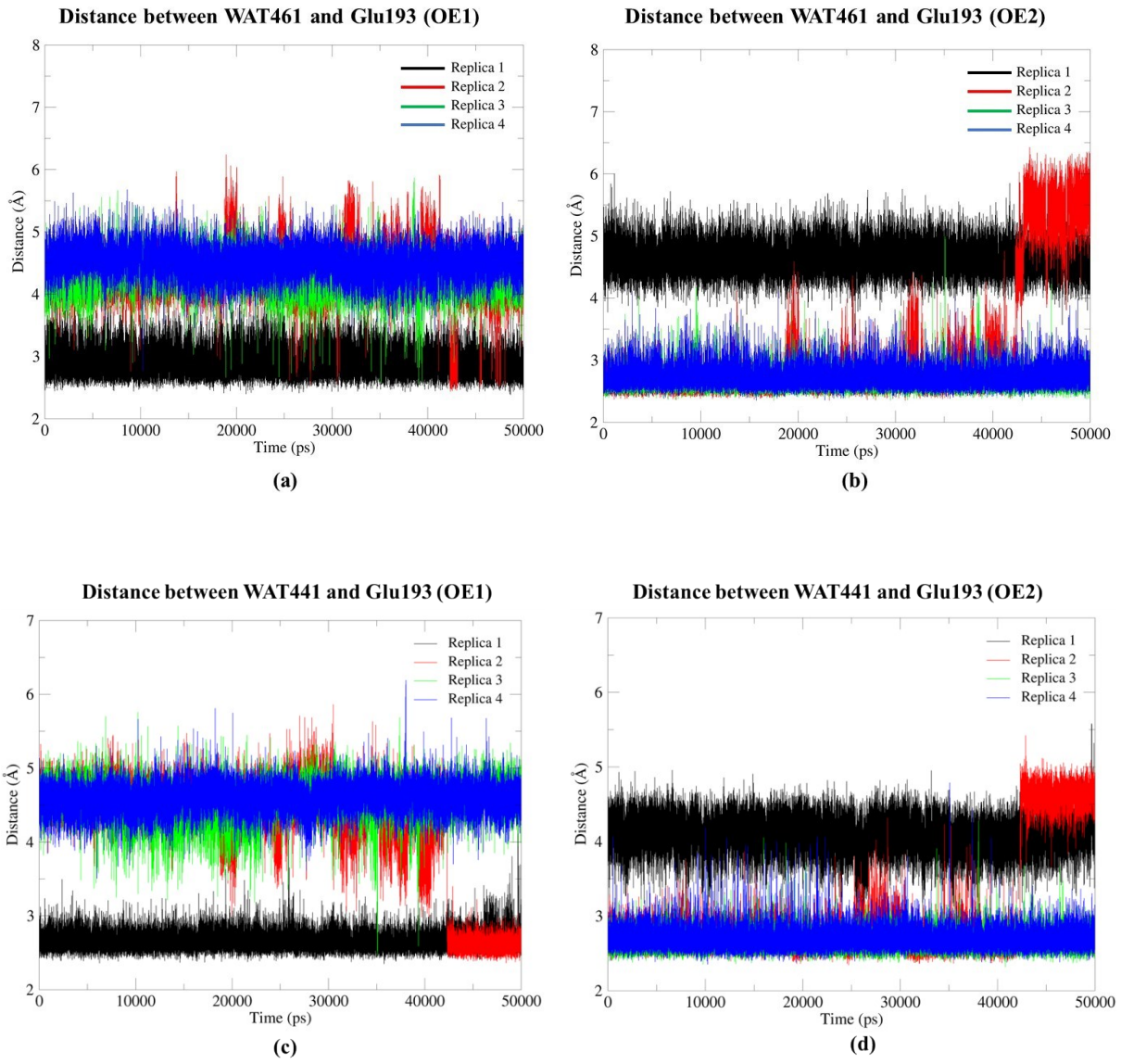

Figure S7. Distance from 4 replicas of 100-ns MD simulations of the ATP -Mg^{2+}-MVK-MVA complex (plotted based on the last 50 ns trajectory) (a) between WAT461 and OE1 of Glu193; (b) between WAT461 and OE2 of Glu193; (c) between WAT441 and OE1 of Glu193; (d) between WAT441 and OE2 of Glu193.

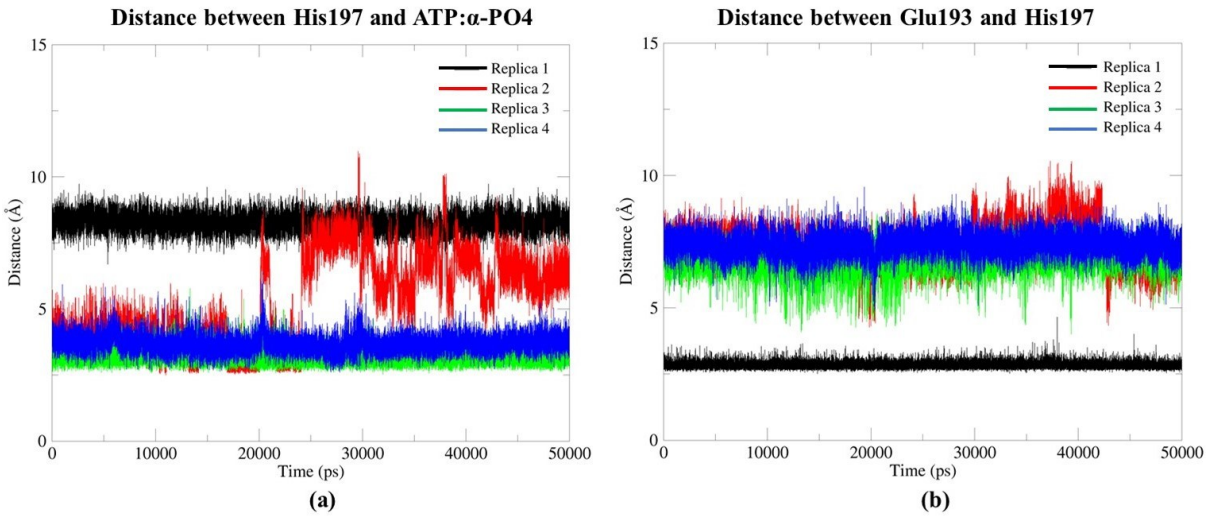

Figure S8. Distance from 4 replicas of 100-ns MD simulations of the ATP -Mg^{2+}-MVK-MVA complex (plotted based on the last 50 ns trajectory) (a) between His197 and the α-phosphate of ATP; (b) between Glu193 and His197.

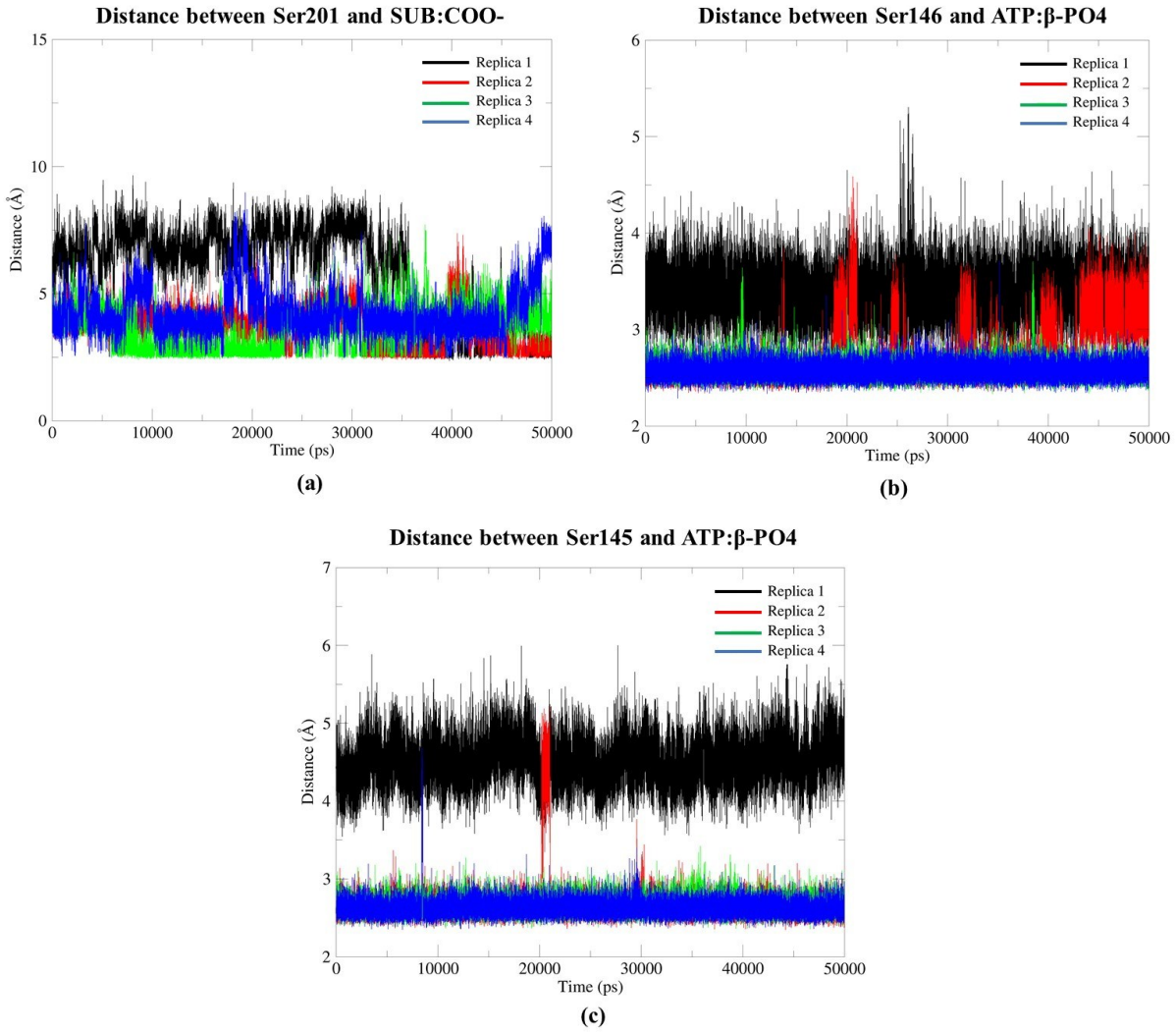

Figure S9. Distance from 4 replicas of 100-ns MD simulations of the ATP -Mg^{2+}-MVK-MVA complex (plotted based on the last 50 ns trajectory) (a) between Ser201 and the carboxylate group of MVA; (b) between Ser146 and the ß-phosphate of ATP; (c) between Ser145 and the ß-phosphate of ATP.

Figure S10. Sequence alignment of kinases in mevalonate pathway using the Clustal Omega webserver developed by the European Bioinformatics Institute. The key residues S145, S146, Glu193 and Ser201 in *Rattus norvegicus* MVK being studied in this research are labelled. Species names are abbreviated as follows: TAC, *Thermoplasma acidophilum* (TAC-M3K: CAC12426.1); Sep, *Staphylococcus epidermidis* (SEP-MDD: AAG02436.1); MEJ, *Arabidopsis thaliana* (ATH-MDD: CAB70999.1); SPO, *Schizosaccharomyces pombe* (SPO-PMK: CAB52264.1); SPN, *Streptococcus pneumoniae* (SPN-PMK: AAK99144.1); RNO, *Rattus norvegicus* (RNO-MVK: AAA41588.1); SCE, *Saccharomyces cerevisiae* (SCE-MVK: CAA29487.1).

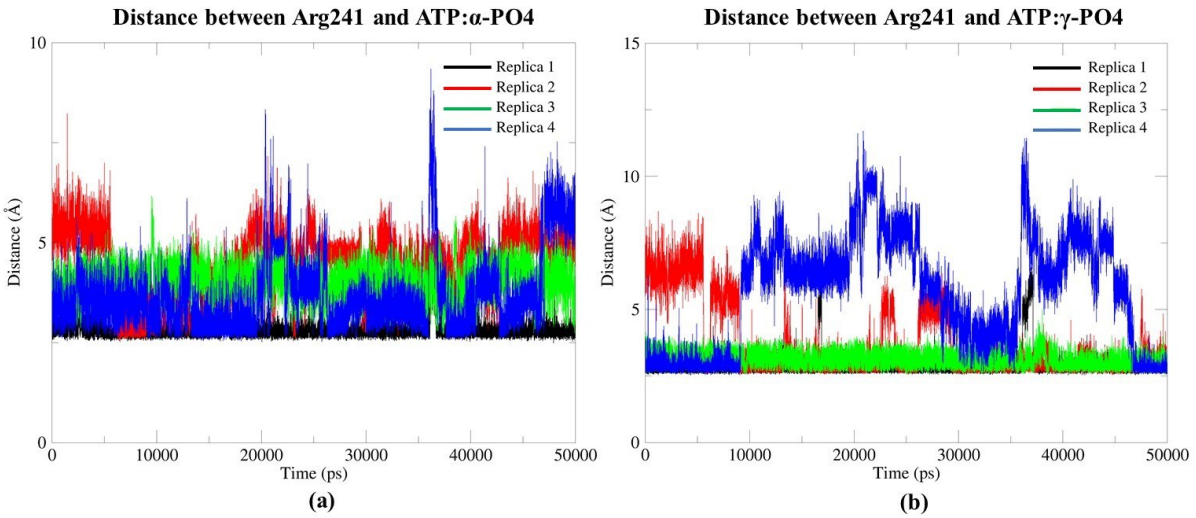

Figure S11. Distance from 4 replicas of 100-ns MD simulations of the ATP-Mg^{2+}-MVK-MVA complex (plotted based on the last 50 ns trajectory) (a) between Arg241 and the α-phosphate of ATP; (b) between Arg241 and the γ-phosphate of ATP.

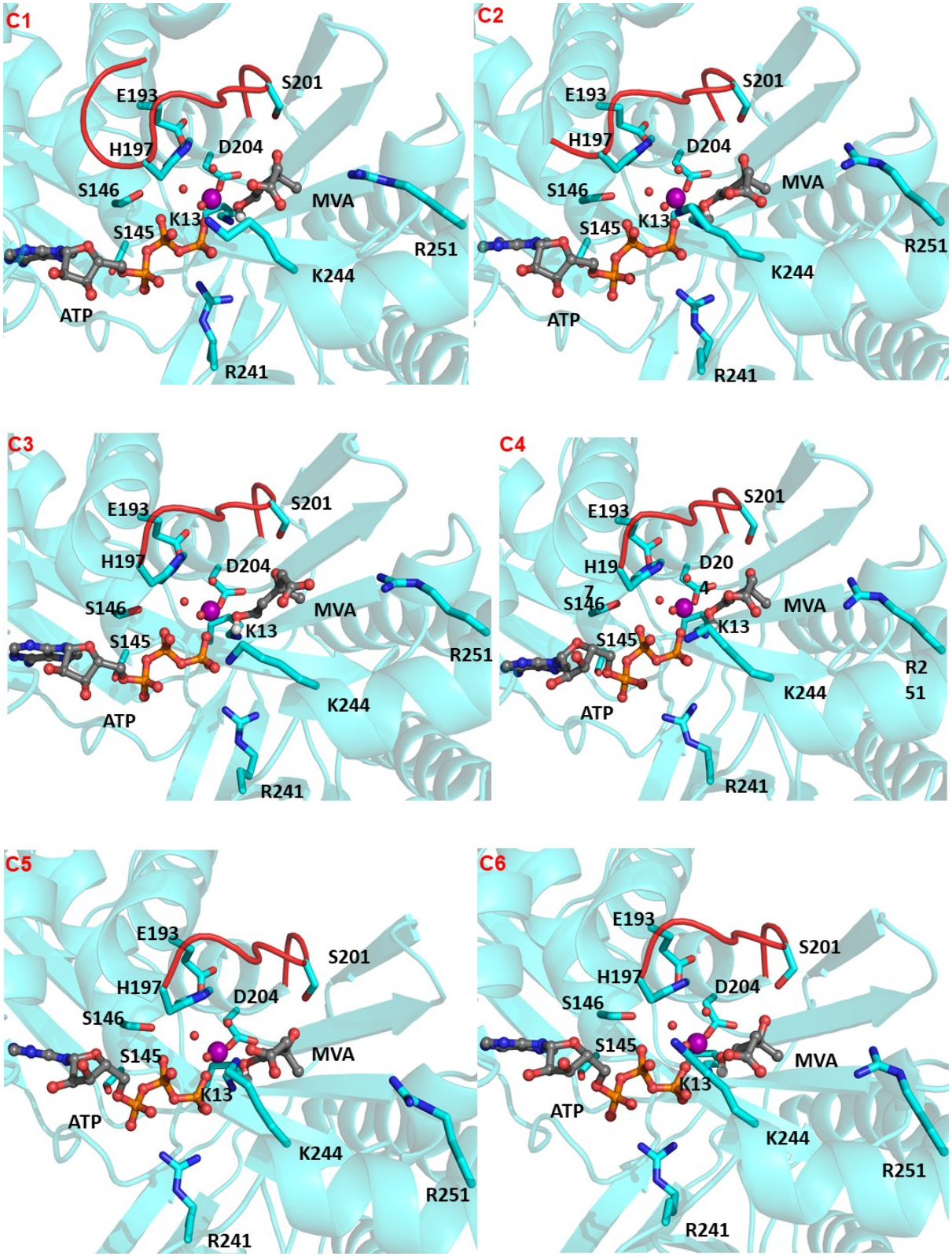
C1
E193
S201
H197
D204
S146
MVA
K13
S145
R251
K244
ATP
R241
C2
E193
S201
H197
D204
MVA
S146
S145
K13
R251
K244
ATP
R241
C3
E193
S201
H197
D204
S146
MVA
K13
S145
R251
K244
ATP
R241
C4
E193
S201
H19
7
D20
4
S146
MVA
K13
S145
R2
51
K244
ATP
R241
C5
E193
S201
H197
D204
S146
MVA
S145
K13
ATP
K244
R251
R241
C6
E193
S201
H197
D204
S146
S145
MVA
K13
ATP
K244
R251
R241

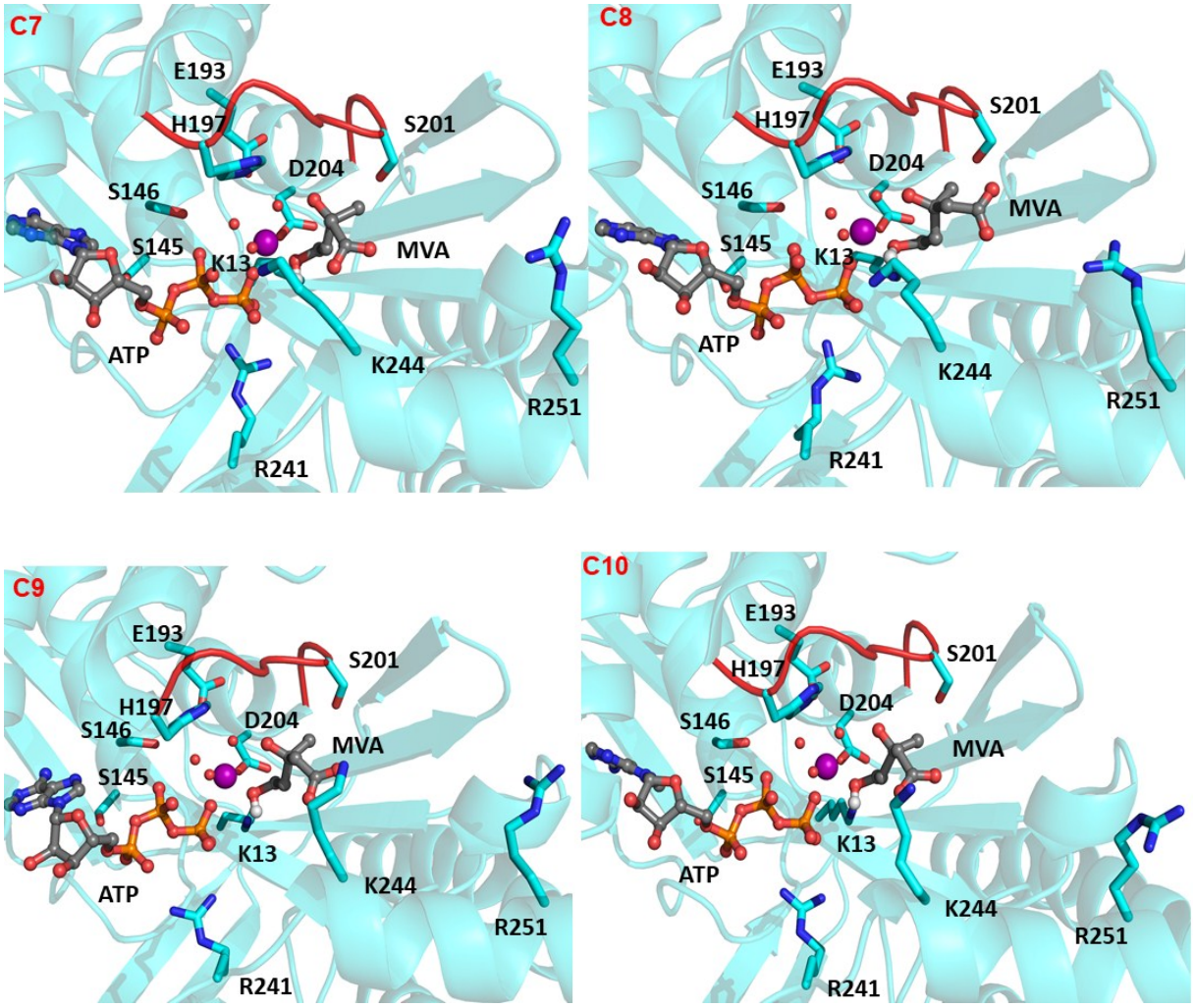

Figure S12. 10 representative structures from cluster analysis of MD simulations of the ATP-Mg^{2+}-MVK-MVA complex.